Electronic Supplementary Material (ESI) for ChemComm.

Supporting Information

Synergetic Effect Enhanced Photoelectrocatalysis

Jingchun Jia, Jie Zhang, Fangfang Wang, Lianhuan Han, Jian-Zhang Zhou, Bing-Wei Mao, Dongping Zhan*

State Key Laboratory of Physical Chemistry of Solid Surfaces, and Department of Chemistry, College of Chemistry and Chemical Engineering, Xiamen University, Xiamen 361005, China

S1 EXPERIMENTAL SECTION

Chemicals and Materials

All chemicals used in the experiments (KBr, $Fe_2(SO_4)_3$, H_2SO_4, ethanol, Rhodamine B) are analytical grade or better provided by Sinopharm Co., China. All aqueous solutions are prepared with deionized water (18.2 MΩ, Milli-Q, Millipore Corp., France). ITO glass slides were washed in an ultrasonic cleaner by isopropanol and deionized water for several times and dried by blowing pure nitrogen gas. The slurry of TiO_2 nanoparticles (average diameter: 20 nm,) is coated on the clean ITO substrate by doctor blading method to form a square TiO_2 spot (500 μm by 500 μm). The ITO slide is sintered at 450 ºC for 2h in a muffle furnace. The area except the TiO_2 spot is encapsulated by a thin insulating film before use. The images relevant to the photoanodes were shown in Fgiure S1.

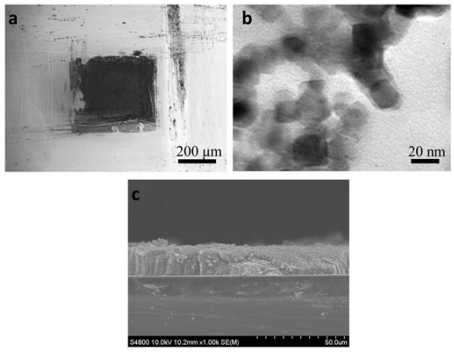

Figure S1. (a) Optical microscopy image of the sqaure TiO_2 spot, (b) transmission electron microscope (TEM) image of TiO_2 Nanoparticles, and (c) scanning electron microscope (SECM) image of the sectional view of TiO_2 photoanode.

Instrumentation and Procedures

The SECM experiments are performed on a CHI 920c workstation (CH Instrument Co., USA). Together with a platinum counter electrode and an Ag/AgCl reference electrode, the photochemically generated Br_2 is detected by a 25-μm-diameter Pt UME (RG: 5). A Xenon lamp (Zolix Co., 0-100 $mWcm^{-2}$) is used as light source.

In the SECM experiments, the tip is fixed at a constant distance above the TiO_2 spot. When the TiO_2 spot is illuminated from the backside of the ITO slide, the steady-state tip current of Br_2 reduction is recorded. The tip potential is held at 0.7 V vs. Ag/AgCl, at which Fe^{3+} is not reduced. From the tip currents at a series of tip-substrate distance, the approach curve of current feedback is plotted. The tip-substrate distance is calibrated by simulating the negative feedback curve of Br^- oxidation (tip potential: 1.0 V vs. Ag/AgCl) without illumination. The principles of the

current feedback are depicted in Figure 1a. The schematic diagram of the SECM measurements are shown in Figure S2.

To identify the autocatalytic effect of the TiO_2/(Fe^{3+}, Br^-) system, the photochemical etching of gallium arsenide (GaAs) as well as photodegradation of Rhodamine B are performed. An optical fiber (diameter: 100 μm) coated with TiO_2 on the end face is fabricated as the SECM tip to generate the echant (Br_2). The tip was positioned on the GaAs wafer with a distance of 1 μm. The etching pits obtained at different photochemical system within same etching time are characterized by confocal laser microscopy (Keyence, VK-X100/X200). As for the degradation of Rhodamine B, a 5-mm-diameter facula was used to illuminate the TiO_2/ITO substrate while the UV-visible spectra were recorded (UV-2550, SHIMADZU Co., 400 -700 nm).

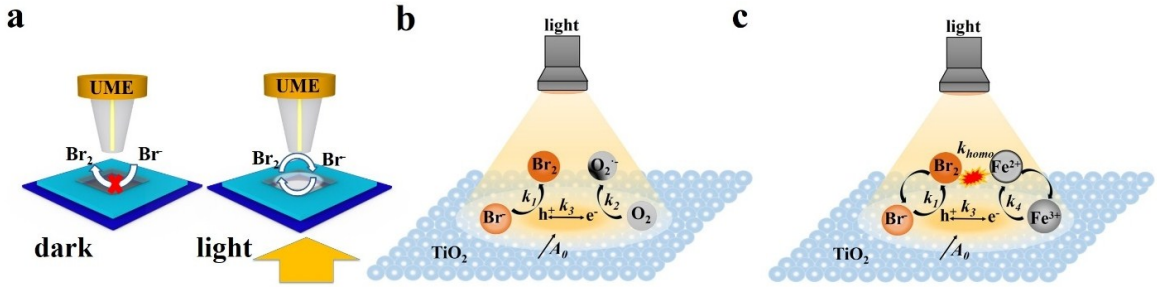

Figure S2. (a) Schematic diagrams of SECM negative (dark) and positive (light) feedback modes of photochemical oxidation of bromide ion, (b) Schematic diagram of TiO_2/(O_2, Br^-) photochemical system, and (c) Schematic diagram of the synergetic effect of TiO_2/ (Fe^{3+}, Br^-) photochemical system.

Experimental feasibility

Since TiO_2 has a high bandgap, the potentials of photogenerated charges are sufficient to be injected into Fe^{3+} and Br^-. It is well known, in the acid solution, the redox couple Fe^{3+}/Fe^{2+} is very reversible. In other words, the photgenerated electron is very easy to be captured by Fe^{3+}. Once this process happens, the whole processes is started. The standard potential of Fe^{3+}/Fe^{2+} and Br_2/Br^- are 0.771 V and 1.087 V vs. SHE. Although the standard potential of O_2/H_2O_2 is 0.695 V vs. SHE. However, the kinetical rate of oxygen reduction is slower than that of Fe^{3+}. Most importantly, the subsequently homogeneous reaction between Br_2 and Fe^{2+} enhanced the mass transfer in the interfacial region. Consenquently, the interfacial transfer of the photogenerated charges are promoted. The the potential of involved species are schemed in Figure S3.

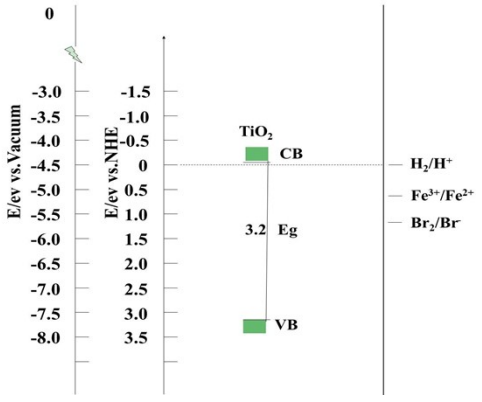

Figure S3 Oxidition levels of Br_2/Br^- and Fe^{3+}/Fe^{2+}, and the band edges of TiO_2.

S2. THEORIES AND SIMULATIONS

The mechanism and numerical analysis of photochemical reduction of oxygen (O_2) have been reported previously.[1] Here, we discuss the photochemical process for the system of TiO_2/(O_2, Br^-), in which O_2 and Br^- serve as the electron and hole acceptor, respectively, but no subsequent homogenous reaction can occur. Figure 1b shows the two charge transfer half-reactions when TiO_2 photoelectrode is illuminated[1,2]:

$$Br^- + h^+ \rightarrow 1/2 Br_2 \tag{1}$$

$$O_2 + e^- \rightarrow O_2^{\bullet -} \tag{2}$$

Here, we define [e^-] and [h^+] as the effective concentration of the transferred electrons and holes, [O_2] and [Br^-] the concentration of O_2 and Br^- at the TiO_2/electrolyte interface, k_1 the rate constant of interfacial hole transfer, k_2 the rate constant of interfacial electron transfer, k_3 the rate constant of charge recombination of electrons and holes, and A_0 the effective flux of the separated electrons and holes when the TiO_2 photoelectrode is illuminated. [3]

At the steady state, the balances for the transferred electrons and holes are given by:

$$\frac{d[e^-]}{dt} = A_0 - k_2[e^-][O_2] - k_3[e^-][h^+] = 0 \tag{3}$$

$$\frac{d[h^+]}{dt} = A_0 - k_1[h^+][Br^-] - k_3[e^-][h^+] = 0 \tag{4}$$

The above equations can be simplified as:

$$[e^-] = \frac{A_0}{k_3[h^+] + k_2[O_2]} \tag{5}$$

$$[h^+] = \frac{A_0}{k_3[e^-] + k_1[Br^-]} \tag{6}$$

Thus, [h^+] can be derived as following:

$$[h^+] = \frac{k_2[O_2]}{2k_3}\left\{\left[\frac{4k_3A_0}{k_1k_2[O_2][Br^-]} + 1\right]^{1/2} - 1\right\} \tag{7}$$

Suppose Reaction (1) is a first-order reaction, the photochemical oxidation rate of Br^- to Br_2 is:

$$r = \frac{k_1k_2[Br^-][O_2]}{2k_3}\left\{\left[\frac{4k_3A_0}{k_1k_2[O_2][Br^-]} + 1\right]^{1/2} - 1\right\} \tag{8}$$

If the effective amount of photogenerated electrons and holes A_0 is large sufficiently, Equation (8) can be simplified as:

$$r = \left(\frac{A_0k_1k_2}{k_3}\right)^{1/2}[Br^-]^{1/2}[O_2]^{1/2} \tag{9}$$

and be rewritten as:

$$r = K_a[Br^-]^{1/2}[O_2]^{1/2} \tag{10}$$

where K_a, equal to $k_1(A_0k_2/k_3)^{1/2}$, is the apparent rate constant of the net charge transfer across the TiO_2/solution interface. It should be noted that, according to the principle of electroneutrality, equation (10) also applies to the interfacial oxygen reduction.

However, it is well known the solubility of O_2 in water is as low as 0.25 mM at 1 atm and 25 ºC after purging the solution with pure O_2 to saturation[4]. It is anticipated that either the mass transfer or the slow kinetics of O_2 reduction would hinder the photochemical conversion rate. We therefore replace the O_2 with Fe^{3+} as the electron acceptor, and the interfacial charge transfer caused by light illumination can be expressed as:

$$Br^- + h^+ \rightarrow 1/2 Br_2 \tag{11}$$

$$Fe^{3+} + e^- \rightarrow Fe^{2+} \tag{12}$$

A distinct feature of the TiO_2/(Fe^{3+}, Br^-) system from that of TiO_2/O_2, Br^- is that a subsequent homogeneous reaction can occur between Br_2 and Fe^{2+} in the electrolyte solution, which regenerates the electron acceptor (Fe^{3+}) and hole acceptor (Br^-) to form a mass transfer loop at the TiO_2/solution interface (Figure S1c):

$$Fe^{2+} + 1/2 Br_2 \rightarrow Fe^{3+} + Br^- \tag{13}$$

Note that it is the Reaction (13) that realizes the autocatalysis of the interfacial charge-transfer processes, and enhances the photochemical conversion rate. Similarly, if the amount of photogenerated electrons and holes are sufficient, the interfacial charge transfer rate can be derived:

$$r = K_b [Br^-]^{1/2} [Fe^{3+}]^{1/2} \tag{14}$$

where, K_b, equal to $k_1(A_0 k_2/k_4)^{1/2}$, is the apparent rate constant of the net charge transfer across the TiO_2/solution interface. Due to the autocatalytic effect, the interfacial concentration of Br^- and Fe^{3+} is relevant to the kinetic rate of Reaction (13). Note that in Equation (10) and (14), the interfacial charge transfer rates, *r*, depend on the interfacial concentration of O_2 or Fe^{3+} in addition to Br^-.

The axisymmetric geometry used to study the interfacial charge transfer of photochemical processes are shown in Figure S2, where the scanning tip is a 25-μm-diameter Pt UME with a RG (defined as the radius ratio between the Pt wire and the sealing glass) of 5 and the substrate is a TiO_2 disc photoelectrode with a radius of 250 μm. The tip potential is held at 0.7 V to collect the photogenerated Br_2. In the steady-state limit, the mass transfer of the reactants and products in the TiO_2/O_2, Br^- system abide by the Fick's 2nd law:

$$\frac{\partial C_i}{\partial t} = D_i \nabla^2 C_i \tag{15}$$

where C_i and D_i is the concentration and diffusion coefficient, respectively, of species *i* in the solution, and *i* represents Br^-, Br_2, O_2, or $O_2^{\bullet -}$.

On the insulative Boundary 1, 4, 5 and 8, there are no normal fluxes for all the species *i*, which are described by

$$\nabla C_i \cdot \vec{n} = 0 \tag{16}$$

where, $\vec{n}$ is the inward unit vector normal to the surface.

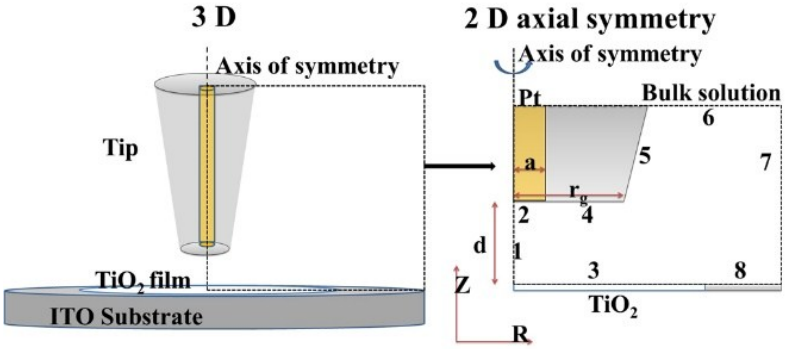

Figure S4. Schematic diagram of the axisymmetric geometry used for the simulation of photochemical processes with a tip radius of 12.5 μm and a RG of 5. The numbers in bold represent the boundary conditions as defined in the text.

On the Boundary 2, the surface concentration of Br^- equals to its bulk concentration ($C^*_{Br^-}$) while the surface concentration of Br_2 is zero:

$$C_{Br^-} = C^*_{Br^-}, \qquad C_{Br_2} = 0 \tag{17}$$

On the Boundary 3, the interfacial fluxes of Br_2 and Br^- are expressed as:

$$-D_{Br_2} \nabla C_{Br_2} \cdot \vec{n} = K_a C_{O_2}^{1/2} C_{Br^-}^{1/2} \tag{18}$$

$$-D_{Br^-} \nabla C_{Br^-} \cdot \vec{n} = -\frac{1}{2} K_a C_{O_2}^{1/2} C_{Br^-}^{1/2} \tag{19}$$

On the boundary 6 and 7, the concentrations of all species equal to their bulk concentrations:

$$C_{Br^-} = C^*_{Br^-}, C_{Br_2} = 0,\ C_{O_2} = C^*_{O_2}, C_{O_2^{\bullet-}} = 0 \quad (20)$$

The current at the Pt UME probe is defined by equation (21):

$$i_{tip} = \int_0^a nFD(\frac{\partial C_{Br_2}}{\partial Z}) \cdot 2\pi RdR \quad (21)$$

where, *n* is the stoichiometric number of electron involved in the tip electrode reaction, and *F* is the faradaic constant.

In the case of the autocatalytic $TiO_2/Fe^{3+},Br^-$ system, the Fick's 2nd law changes due to the subsequent homogeneous reaction:

$$\frac{\partial C_{Br^-}}{\partial t} = D_{Br^-}\nabla^2 C_{Br^-} + K_{homo} C_{Br_2} C_{Fe^{2+}} \quad (22)$$

$$\frac{\partial C_{Br_2}}{\partial t} = D_{Br_2}\nabla^2 C_{Br_2} - K_{homo} C_{Br_2} C_{Fe^{2+}} \quad (23)$$

$$\frac{\partial C_{Fe^{3+}}}{\partial t} = D_{Fe^{3+}}\nabla^2 C_{Fe^{3+}} + K_{homo} C_{Br_2} C_{Fe^{2+}} \quad (24)$$

$$\frac{\partial C_{Fe^{2+}}}{\partial t} = D_{Fe^{2+}}\nabla^2 C_{Fe^{2+}} - K_{homo} C_{Br_2} C_{Fe^{2+}} \quad (25)$$

The boundaries are similar as long as the O_2 and $O_2^{\bullet-}$ are substituted by Fe^{3+} and Fe^{2+}. K_{homo} is the rate constant in Equation (14), which is simulated based on the experiment results.

A commercial finite element modelling package (COMSOL Multiphysics 4.3b) was employed to simulate the above photochemical processes. The involved constant are: $D_{Br2} = 1.77 \times 10^{-9}$ m^2 s^{-1},[5] $D_{O2} = 1.98 \times 10^{-9}$ m^2 s^{-1},[6] $D_{Fe}^{3+} = 2.5 \times 10^{-9}$ m^2 s^{-1}.[7] Fitting theoretical approach curves to experimental ones, the kinetics of the photoinduced interfacial charge transfer and the subsequently homogeneous reaction can be derived.

S3 Photochemical degradation of Rhodamine B

If a competing reaction pathway is introduced into the $TiO_2/(Fe^{3+}, Br^-)$ system, three possible cases will be taken place: (1) If the reaction rate between Br_2 and Rhodamine B is much faster than that between Br_2 and Fe^{2+}, the produced Br_2 will react mainly with Rhodamine B. it results in a net consumption of Fe^{3+}, which may make the interfacial charge transfer ceased. (2) If the reaction rate between Br_2 and Rhodamine B is much slower than that between Br_2 and Fe^{2+}, Rhodamine B will hardly be degraded. (3) If the reaction rate between Br_2 and Rhodamine B is comparable with that between Br_2 and Fe^{2+}, a new equilibrium should be established for the whole system. In this case, new mass and charge balance will be achieved for both the precursors of Fe^{3+} and Br^-. Comparing Figure 4c and Figure 4d, it is essential to use a sufficient concentration of Fe^{3+} to maintain the mass balance and accelerated the degradation process. It should be noted that in the degradation and etching experiment the solution is not degassed. Moreover, it is well known that Fe^{2+} is not stable in aqueous solution, and very easy to lose an electron to the photogenerated Br_2, the dissolved O_2, or the directly to the illuminated TiO_2 to maintain the balance of the precursor Fe^{3+}. From the results shown in Figure 4 and Figure 5 in the main text, we are inclined to consider that the Case 3 is mostly happened. Similar analysis is applied to the etching of GaAs wafer. The schematic diagram of the mechanisms is shown in Figure S5b.

a

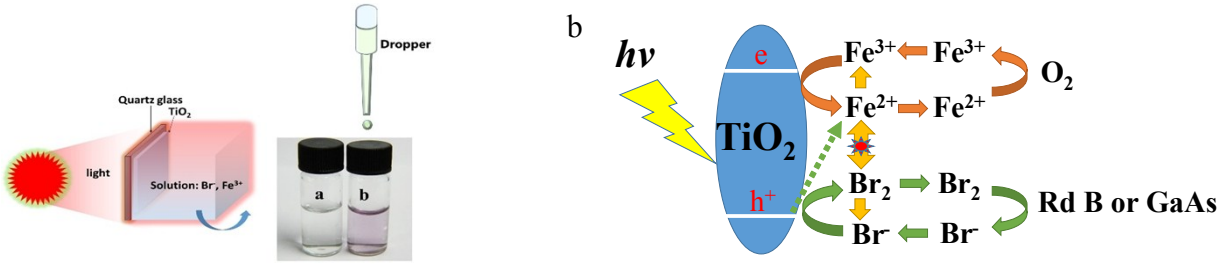

Figure S5 (a) TiO_2/(1.0 mM Fe^{3+}, 5.0 mM Br^-) photochemical system is capable of producing net bromine. Bottle a: before illumination; Bottle b: After 20 minutes' illumination. When a drop of N,N-dimethyl-p-phenylenediamine (DPD) is added in, the color of the electrolyte changes into pink. (b) the mechanisms for photodegradation of Rhodamine B(RbB).

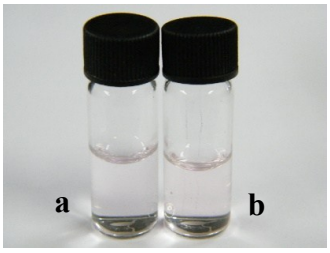

Figure S6 (a) The photodegradation of Rhodamine B by TiO_2/(50 mmol H_2SO_4, 5 mmol KBr, 1 mmol Fe^{3+}).The light intensity of Xenon light is 50 $mW \cdot cm^{-2}$, the illumination time is 60 min and the diameter of illumination area of TiO_2 photoelectrode is 5 mm; (b) The direct reaction between Rhodamine B and Br_2 in the solution containing 50 mmol H_2SO_4. This result elucidate Br_2 has the capability to degrade Rhodamine B.

Figure S7 (a)-(d) are photodegradation results of Rhodamine B which corresponding to the (a)-(d) of Figure 4 in the text. (e) the solution before illumination.

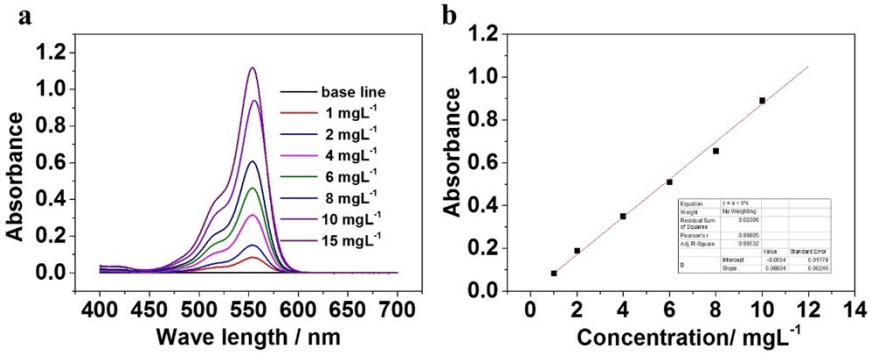

Figure S8 The calibration curve of the concentration of Rhodamine B.

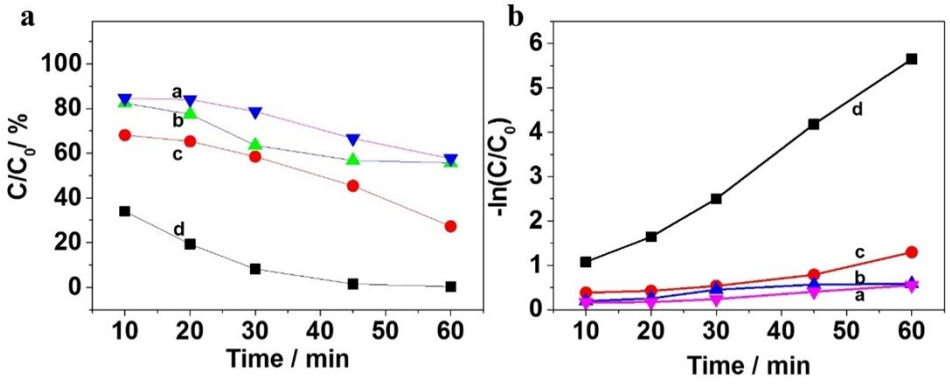

Figure S9 The calculation results of the date shown in Figure 4 in the text based on the calibration curve shown in Figure S8. From the linear relationship between -ln(C/Co) and illumination time, the photodegradation rates are derived.

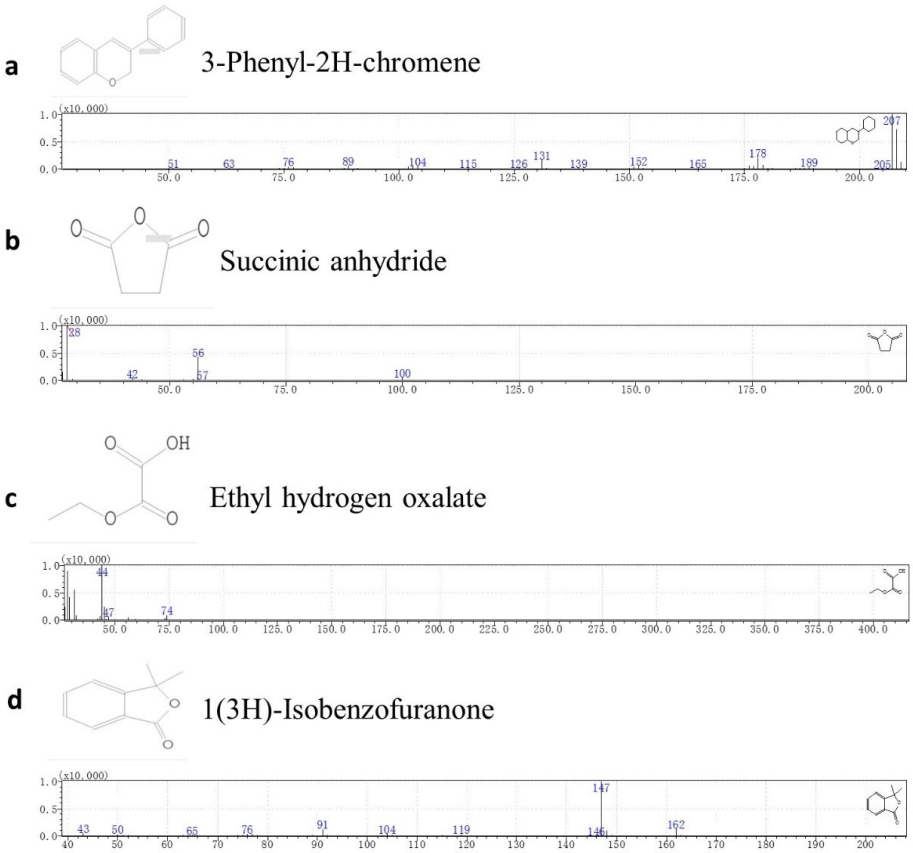

Figure S10 Mass spectra of degradation products, (a) 3-Phenyl-2H-chromene, (b) Succinic anhydride-2,5-Furandione, (c) Ethyl hydrogen oxalate, (d) 1(3H)-Isobenzofuranone. The results show that no bromination reaction but homogeneous redox reaction between Rhodamine B and Br_2 occurs. There are no new pollutants, i.e., organic bromides, produced during the photodegradation process. The results indicate a green chemistry.

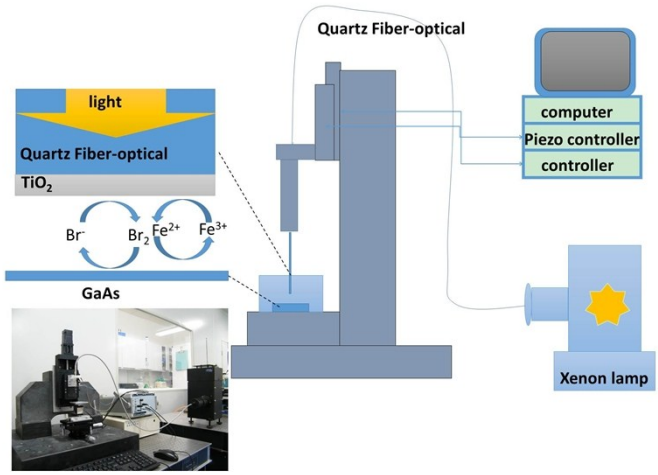

Figure S11 The home made SECM instrument with an optical fiber tip coated with TiO_2 nanoparticles for the etching process on GaAs wafer.

REFERENCES

(1) Kesselman, J. M.; Shreve, G. A.; Hoffmann, M. R.; Lewis, N. S. *J. Phys. Chem.* **1994**, *98*, 13385.
(2) Reichman, B.; Byvik, C. E. *J. Phys. Chem.* **1981**, *85*, 2255.
(3) Fonseca, S. M. M. C. d., University of Warwick, 2002.
(4) Fonseca, S. M.; Barker, A. L.; Ahmed, S.; Kemp, T. J.; Unwin, P. *PCCP* **2004**, *6*, 5218.
(5) Zhang, J.; Jia, J.; Han, L.; Yuan, Y.; Tian, Z.-Q.; Tian, Z.-W.; Zhan, D. *The J. Phys. Chem. C* **2014**, 118, 18604-18611.
(6) Han, P.; Bartels, D. M. *The J.Phys. Chem.***1996**, *100*, 5597.
(7) Amira, S.; Spångberg, D.; Probst, M.; Hermansson, K. *The J.Phys. Chem. B* **2004**, *108*, 496.